Control of a 9-DoF Wheelchair-Mounted Robotic Arm System

Redwan Alqasemi and Rajiv Dubey
University of South Florida
4202 E. Fowler Ave, ENB 118
Tampa, FL 33620
+1(813)974-2280
ralqasemi@gmail.com, dubey@eng.usf.edu

ABSTRACT
A wheelchair-mounted robotic arm (WMRA) system was designed and built to meet the needs of mobility-impaired persons with limitations of upper extremities, and to exceed the capabilities of current devices of this type. The control of this 9-DoF system expands on the conventional control methods and combines the 7-DoF robotic arm control with the 2-DoF power wheelchair control. The 3-degrees of redundancy are optimized to effectively perform activities of daily living (ADLs) and overcome singularities, joint limits and some workspace limitations. The control system is designed for teleoperated or autonomous coordinated Cartesian control, and it offers expandability for future research, such as voice or sip and puff control operations and sensor assist functions.

Keywords
Rehabilitation, Redundancy, Robot, Wheelchair, ADL.

1. INTRODUCTION
A wheelchair mounted robotic arm can enhance the manipulation capabilities of individuals with disabilities that are using power wheelchairs, and reduce dependence on human aides. Unfortunately, most WMRAs have had limited commercial success due to poor usability and low payload. It is often difficult to accomplish many of the Activities of Daily Living (ADL) tasks with the WMRAs currently on the market due to its physical and control limitations and its control independence of the wheelchair's control system. This project attempts to surpass available commercial WMRA devices by offering an intelligent system that combines the mobility of the wheelchair and the manipulation of a newly designed arm in an effort to improve performance, usability, control and reduce mental load on the user while maintaining cost competitiveness.

According to the latest data from the US Census Bureau Census Brief of 1997 [1] showed that one of every five Americans had difficulty performing functional activities (about 53 million), half of them were considered to have severe disabilities (over 26 million). This work focuses on people who have limited or no upper extremity mobility due to spinal cord injury or dysfunction, or genetic predispositions. Robotic aides used in these applications vary from advanced limb orthosis to robotic arms [2]. Persons that can benefit from these devices are those with severe physical disabilities, which limit their ability to manipulate objects. These devices increase self-sufficiency, and reduce dependence on caregivers. The two commercially available WMRAs lack the integration of the robotic arm controller with the wheelchair controller, and that leads to an increased mental load on the user. Combining the control of both the wheelchair and the robotic arm would decrease this mental burden and improve the usability of the device.

The main objective of this work is to develop and optimize a control system that combines the manipulation of the newly designed 7-DoF robotic arm and the mobility of a modified 2-DoF wheelchair in a single control algorithm. Redundancy resolution is to be optimally solved to avoid singularities and joint limits as well as to allow larger wheelchair or manipulator motion depending on the proximity to the goal. The controller is capable of moving autonomously or using teleoperation.

2. BACKGROUND
There are several designs of workstation-based robotic arm systems, but WMRAs combine the idea of workstation and mobile-base robots to mount a manipulator arm onto a power wheelchair. The most important design consideration of where to mount a robotic arm in a power wheelchair is the safety of the operator [3]. There have been several attempts in the past to create commercially viable wheelchair mounted robotic arms, including the two commercial WMRAs: Manus and Raptor.

The Manus manipulator, manufactured by Exact Dynamics, available since the early 1990s [4], can be programmed in a manner comparable to industrial robotic manipulators. A picture of Manus mounted onto a Permobil Max90 wheelchair is shown in Figure 1. It is a 6 DoF arm, with servomotors all housed in a cylindrical base. Besides the fact that it is controlled independent of the wheelchair control, the current controller allows for Cartesian control, but when it comes close to a singularity, it stops and waits for the user to move it in a different direction. This kind of control increases the cognitive load on the user.

Another production WMRA is the Raptor, manufactured by Applied Resources [5], as shown in Figure 2, which mounts to the right side of the wheelchair. This manipulator has four degrees of freedom plus a planar gripper. The user directly controls the arm with either a joystick or a keypad controller. Because the Raptor does not have encoders, the manipulator cannot be controlled in Cartesian coordinates. This compromise was done to minimize the overall system cost, but it highly decreases the usability of the arm.

Weighted least norm solution method was used by Chan et al [6] to penalize the motion of some joints over others. This method

can be used in the case of WMRAs to make the wheelchair motion as a secondary motion when needed. The combination of mobility and manipulation in a robotic arm has been studied by researchers in the form of a mobile platform that carries a robotic arm. Chung, et al [7] resolved the kinematic redundancy by decomposing the mobile manipulator into two different subsystems, the mobile platform and the manipulator. Each one of these subsystems is controlled independently with an interaction algorithm between the two controllers.

Figure 1: Manus arm

Figure 2: Raptor arm

Mirosaw [8] used external penalty functions to enforce the holonomic manipulability and collision avoidance. His results showed continuous velocities near obstacles. An extension to different redundancy resolution schemes has been proposed by Luca [9] to include the representation of mobile platforms in the jacobian. His simulation showed consistent results in simulation.

3. MOTION CONTROL OF THE 9-DoF WMRA SYSTEM

3.1 Wheelchair Motion

The differential drive used in power wheelchairs represents a 2-DoF system that moves in plane [10]. Assuming that the manipulator is mounted on the wheelchair with L2 and L3 offset distances from the center of the differential drive across the x and y coordinates respectively, the mapping of the wheels' velocities to the end-effector velocities along its coordinates is defined by:

$$\dot{q}_c = J_c \cdot J_W \cdot V_c \quad \text{, where:} \tag{1}$$

$$\dot{q}_c = \begin{bmatrix} \dot{x} & \dot{y} & \dot{z} & \dot{\alpha} & \dot{\beta} & \dot{\phi} \end{bmatrix}^T \quad , \quad V_c = \begin{bmatrix} \dot{\theta}_l \\ \dot{\theta}_r \end{bmatrix} \quad ,$$

$$J_c = \begin{bmatrix} I_2 & \begin{bmatrix} -(P_{xg} \cdot S\phi + P_{yg} \cdot C\phi) \\ P_{xg} \cdot C\phi - P_{yg} \cdot S\phi \end{bmatrix} \\ [0]_{2x2} & [0]_{3x1} \\ [0]_{2x2} & 1 \end{bmatrix}, \text{ and}$$

$$J_W = \frac{l_5}{2} \begin{bmatrix} c\phi_c + \frac{2}{l_1}(l_2 s\phi_c + l_3 c\phi_c) & c\phi_c - \frac{2}{l_1}(l_2 s\phi_c + l_3 c\phi_c) \\ s\phi_c - \frac{2}{l_1}(l_2 c\phi_c - l_3 s\phi_c) & s\phi_c + \frac{2}{l_1}(l_2 c\phi_c - l_3 s\phi_c) \\ \frac{-2}{l_1} & \frac{2}{l_1} \end{bmatrix}$$

Where P_{xg} and P_{yg} are the x-y coordinates of the end-effector based on the arm base frame, Φ is the angle of the arm base frame, and L5 is the wheels' radius. The above Jacobian can be used to control the wheelchair with the jacobian of the arm after combining them together.

3.2 The 7-DoF Arm Motion

From the DH parameters specified earlier publications [11], the 6x7 Jacobian that relates the joint rates to the Cartesian speeds of the end effector based on the base frame is generated according to Craig's notation [12]:

$$\dot{r} = J_A \cdot V_A \tag{2}$$

where: $\dot{r} = \begin{bmatrix} \dot{x} & \dot{y} & \dot{z} & \dot{\alpha} & \dot{\beta} & \dot{\gamma} \end{bmatrix}^T$ is the task vector, and $V_A = \begin{bmatrix} \dot{\theta}_1 & \dot{\theta}_2 & \dot{\theta}_3 & \dot{\theta}_4 & \dot{\theta}_5 & \dot{\theta}_6 & \dot{\theta}_7 \end{bmatrix}^T$ is the joint velocities vector. Numerical solutions are implemented using the Jacobian to follow the user directional motion commands or to follow the desired trajectory. Manipulability measure [13] is used as a factor to measure how far is the current configuration from singularity. This measure is defined as:

$$w = \sqrt{\det(\underline{J_A} * \underline{J_A^T})} \tag{3}$$

Redundancy is resolved in the program structure using Pseudo Inverse of the Jacobian [13], and singularity is avoided by maximizing the manipulability measure. Since this method carries a guaranteed valid solution only at a singular configuration and not around it, the results carried high joint velocities when singularity is approached. We then decided to use S-R Inverse of the Jacobian [14] to give a better approximation around singularities, and use the optimization for different subtasks. S-R Inverse of the Jacobian is used to carry out the inverse kinematics:

$$\underline{J_A^*} = \underline{J_A^T} * (\underline{J_A} * \underline{J_A^T} + k * \underline{I_6})^{-1} \tag{4}$$

where I_6 is a 6x6 identity matrix, and k is a scale factor. It has been known that this method reduces the joint velocities near singularities, but compromises the accuracy of the solution by increasing the joint velocities error. Choosing the scale factor k is critical, if it is too high, the error will be too high and the system might destabilize, and if it is too small, the joint rates will go too high, and the system might destabilize. Since the point in using this factor is to give approximate solution near and at singularities, an adaptive scale factor is updated at every time step to put the proper factor as needed:

$$k = \begin{cases} k_0 * (1 - \frac{w}{w_0})^2 & for \quad w < w_0 \\ 0 & for \quad w \geq w_0 \end{cases} \tag{5}$$

where w_0 is the manipulability measure at the start of the boundary chosen when singularity is approached, and k_0 is the scale factor at singularity. It was found that the optimum values of w_0 and k_0 for our system are 0.02 and 0.35×10^{-3} respectively.

Now that the singularity is taken care of using the S-R Inverse of the Jacobian, we can use the joint redundancy to optimize for a secondary task as follows:

$$\underline{V_d} = \underline{J_A^*} * \underline{\dot{r}_d} + (\underline{I_7} - \underline{J_A^*} * \underline{J_A}) * \underline{f} \tag{6}$$

where f is a 7x1 vector representing the secondary task. That task can either be the desired trajectory in the case of pre-set task execution, or it can be a criterion function that represents the potential energy to be minimized.

3.3 The 9-DoF WMRA System Motion

Combining the two subsystems together by means of jacobian augmentation [9] can give the flexibility of using conventional control and optimization methods without compromising the total system coordinated control. In the case of combined control, let the task vector be:

$$r = f(q_c, q_A) \tag{7}$$

Differentiating (7) with respect to time gives:

$$\dot{r} = \frac{\partial f}{\partial q_c} V_c + \frac{\partial f}{\partial q_A} V_A = J_c J_W V_c + J_A V_A$$

$$= \begin{bmatrix} J_c J_W & J_A \end{bmatrix} \begin{bmatrix} V_c \\ V_A \end{bmatrix} \quad \text{or, } \dot{r} = J \cdot V \tag{8}$$

Solving (8) in conventional methods is now possible. Choosing the Projected Gradient method, which proved effective, gives:

$$\begin{bmatrix} V_W \\ V_A \end{bmatrix} = J^* \dot{r} + \left(I - J^* J\right) V_0 \tag{9}$$

Where $V_0 = a \nabla_q H(q)$ for conventional arms, and H(q) is the optimization criteria y=H(q). The existence of the mobile platform means that V_o may not exist for non holonomic constraint such as that of the wheelchair. To go around this limitation [9] proposed the following: Differentiate the optimization criteria function "H" with respect to time as follows:

$$\dot{y} = \dot{H}(q) = \frac{\partial H}{\partial q_c} V_c + \frac{\partial H}{\partial q_A} V_A$$

$$= \nabla_q^T H \begin{bmatrix} J_W & 0 \\ 0 & I \end{bmatrix} \begin{bmatrix} V_c \\ V_A \end{bmatrix} \tag{10}$$

In this case, the value of V_H that improves the objective function is:

$$V_H = \pm a \begin{bmatrix} J_W^T & 0 \\ 0 & I \end{bmatrix} \nabla_q H(q) \equiv V_0 \tag{11}$$

and that velocity vector can be used for optimization. This gives a good representation of the arm joints' velocities and the wheels' velocities of the wheelchair.

Weighted Least Norm solution can also be used as proposed by [6]. In order to put a motion preference of one joint rather than the other (such as the wheelchair wheels and the arm joints), a weighted norm of the joint velocity vector can be defined as:

$$\left|V\right|_W = \sqrt{V^T W V} \tag{12}$$

where W is a 9X9 symmetric and positive definite weighting matrix, and for simplicity, it can be a diagonal matrix that represent the motion preference of each joint of the system. For the purpose of analysis, the following transformations are introduced:

$$J_W = J W^{-1/2} \text{ and } V_W = W^{-1/2} V \tag{13}$$

From (12) and (13), it can be shown that the weighted least norm solution is:

$$V_W = W^{-1} J^T \left(J W^{-1} J^T\right)^{-1} \dot{r} \tag{14}$$

The above method has been used in simulation of the 9-DoF WMRA system with the nine state variables (V_d) that represent the seven joint velocities of the arm and the two wheels' velocities of the power wheelchair. It was found that latter two state variables are of limited use since they tend to unnecessarily rotate the wheelchair back and forth during a long forward motion due to their equal weights. Changing the weights of these two variables will only result in a preference of one's motion over the other.

Two new state variables were introduced out of the wheels' velocities, which represent the pure angular speed of the wheelchair when both wheels run at equal but opposite velocities and the pure forward speed of the wheelchair when both wheels run at equal velocities as follows:

$$\dot{\phi} = \frac{2 l_5 \dot{\theta}_r}{l_1}, \quad and \quad \dot{X} = l_5 \dot{\theta}_r \tag{15}$$

The combination of the above two variables would be sufficient to describe any forward and rotational motion of the wheelchair. Having these two state variables in (V) instead of the wheels' velocities give a greater advantage in controlling the preferred rotation or translation of the wheelchair. The wheelchair's jacobian in (1) is changed for the new state variables before augmenting it to the arm's jacobian, and the results were much better in terms of valuable control. The new state variables are:

$$V = \begin{bmatrix} \dot{\theta}_1 & \dot{\theta}_2 & \dot{\theta}_3 & \dot{\theta}_4 & \dot{\theta}_5 & \dot{\theta}_6 & \dot{\theta}_7 & \dot{X} & \dot{\phi} \end{bmatrix}^T \tag{16}$$

Care must be taken when implementing the above change in the controller algorithm since one of the state variables (the forward motion of the wheelchair) carry linear velocity units, which are different from the rest of the state variables, which carry angular velocity units.

4. DESIGN OF THE NEW ARM

4.1 Hardware Design of the Arm

An entirely new WMRA was developed, designed and built. The goal was to produce an arm that has better manipulability, greater payload, and easier control than current designs. As found in previous research [15], side mounting is preferable overall because it provides the best balance between manipulability and unobtrusiveness. This mounting location allows the arm to be stowed by folding it back and then wrapping the forearm behind the seat. This helps avoid the stigma that these devices can bring. It virtually disappears when not in use, especially when the arm is painted to match the chair. However, care must be taken to prevent widening of the power chair. Our arm only increases chair width by 7.5cm.

This manipulator is intended for use in Activities of Daily Living (ADL), and for job tasks of a typical office environment. As such, it is important that the arm be strong enough to move objects that

are common in these environments. Approximately 4 kg mass is set as the upper limit for a typical around-the-house object that must be manipulated. This was set as the baseline payload for the arm at full horizontal reach at rest. Then, an extra margin of 2 kg was added to allow for a choice of an end-effector.

Reconfigurable arm lengths allow greater leverage on the engineering input, as a single basic design may be adapted to numerous applications. This is only practical with electric drive and actuator placement directly at each joint.

In the power wheelchair industry, a 24-volt lead-acid battery pack is standard, and is the natural choice for the power supply of a WMRA with minimum power consumption. To have a widespread adoption of these devices, reasonable cost is important. The target was to be in the mid-range of commercially available systems in terms of cost. Extra degrees of freedom help improve manipulability. This is evidenced by the considerable increase going from Raptor's 4 DoF to the 6 DoF of MANUS. Our new design incorporates 7 joints, allowing full pose control even in difficult regions of the workspace, such as reaching around the wheelchair, or up to a high shelf.

The arm is a 7-DoF design, using 7 revolute joints. It is anthropomorphic, with joints 1, 2 and 3 acting as a shoulder, joint 4 as an elbow, and joints 5, 6 and 7 as a wrist as shown in Figure 3. The 3 DoF shoulder allows the elbow to be positioned anywhere along a spherical surface, whereas with the Raptor arm, elbow movement is limited to a circle. Throughout the arm, adjacent joint axes are oriented at 90 degrees as shown in Figure 4. This helps to meet two goals: mechanical design simplicity and kinematic simplicity with low computational cost. All adjacent joint axes intersect, also simplifying the kinematics. The basic arrangement for each joint is a high-reduction gearhead, a motor with encoder and spur-gear reduction, and a bracket that holds these two parts and attaches to the two neighbouring links.

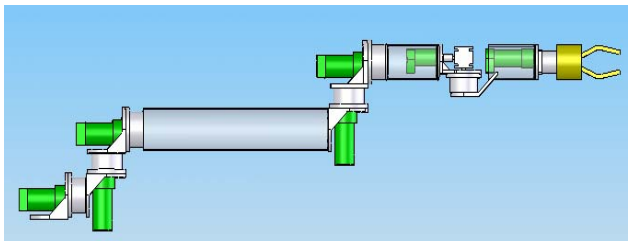

Figure 3: Complete SolidWorks model of the arm

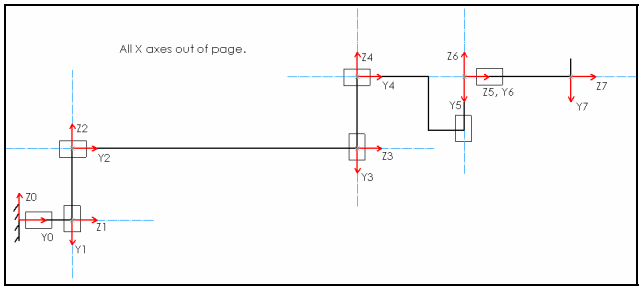

Figure 4: Kinematic diagram, with link frame assignments

4.2 Hardware Design of the Controller

As shown in Figure 5, PIC-SERVO SC controllers (C1 through C7) that support the DC servo actuators (J1 through J7) were chosen. At 5cm x 7.5cm, this unit has a microprocessor that drives the built-in amplifier with a PWM signal, handles PID position and velocity control, communicates with RS-485, and can be daisy-chained with up to 32 units. It also reads encoders, limit switches, an 8 bit analogue input, and supports coordinated motion control. Data for the entire arm is interfaced to the main computer using a single serial link. The PIC-Servo SC controllers use RS-485, and a hardware converter interfaces this with the RS-232 or a USB port on the host PC. A timer has been utilized to cut the arm's power off after a preset time to minimize power consumption while not in use. An emergency stop button is placed to cut the power off the motors and leave the logic power on so that the system can be diagnosed without rebooting.

The current host PC is an IBM laptop, running Windows XP. However, the communications protocol is simple and open, and could be adapted to virtually any hardware/software platform with an RS-232 or USB port. Currently, the tested user interfaces are the keyboard and a SpaceBall controller.

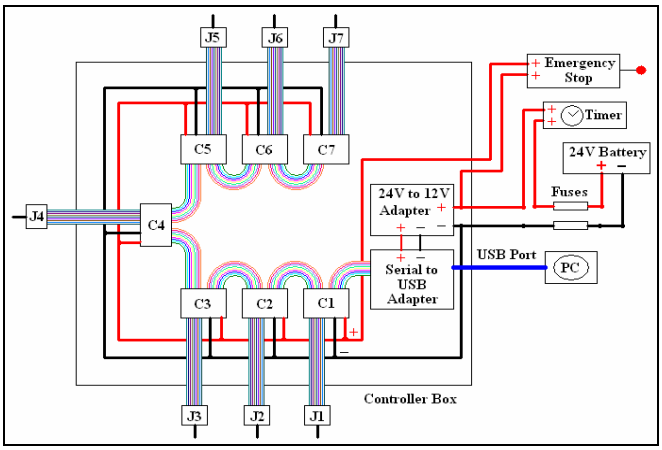

Figure 5: Control system circuitry

4.3 Control Modes

Different pre-set ADL tasks were chosen to be programmed into the control system. These tasks range from reaching/ carrying/ placing objects to turning on/off switches.

The control of the new WMRA is designed to satisfy two main modes. The first mode is the scaled teleportation mode; this mode is for the user to control the arm in real time using a joystick, a keyboard, a space ball, a haptic device, head/foot switches, sip and puff, touch screen, or the BCI 2000 system that reads certain electromagnetic pulses out of the brain after excitation by several choices on a visual screen. In this context, trajectory generation is not required since the user is specifying the direction of the end effector motion at each instance rather than specifying a goal position. The second mode is the autonomous mode, where a goal is specified either directly by the user or by the sensory feedback. In this case, a trajectory needs to be generated and followed. This trajectory is generated using a 3rd degree polynomial with blending [12] for smooth velocities. This mode is used for pre-specified ADL tasks to be executed when the user needs these tasks.

Sensory suite including a camera, a laser range finder, and proximity sensors will be added at the end effector and around the wheelchair to allow autonomous and semi autonomous control of

the system. Advanced software that recognizes user-selected objects will enable the system to use assist functions that enhance the system's capabilities and reduce the user's mental load. This will ease what could be a tedious process for the user.

Scaled teleoperation control system is implemented to filter out the involuntary user input or signal noise and to scale up the intended user input for the required task. With the integration of the scaling and the sensory input in the control structure, the system can be very effective in avoiding unintentional motion of the wheelchair-robot system due to user errors. It can also lead to a better user safety measures that are important for users with disabilities.

The details on the above user interfaces, sensory suite and intelligence algorithms are out of the scope of this paper, and will be published in later publications.

4.4 The Wheelchair

Figure 6 shows the WMRA system installed on the modified wheelchair "Action Ranger X Storm Series". The wheelchair has been modified by adding an incremental encoder on each one of the wheels.

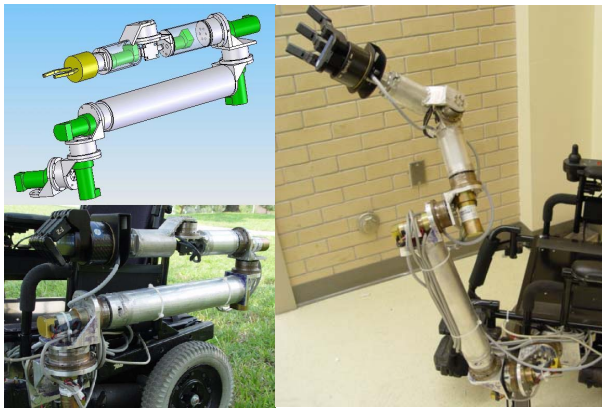

Figure 6: WMRA SolidWorks models and the built device

The controller module of the wheelchair has also been modified using TTL compatible signal conditioner and a DA converter so that the signal going to the wheels can be controlled using the same PIC-Servo SC controllers used in the arm. The only difference is that the output from this control board used for the wheelchair is the PWM signal rather than the amplified analogue signal.

5. SIMULATION REDULTS

The control system of the 9-DoF WMRA system is implemented in simulation using Matlab 7.0.4 with Virtual Reality toolbox installed on a PC running Windows XP. Figure 7 shows the end-effector's position and orientation during simulation as it moves from the initial to the commanded point in the workspace.

Several methods are being tested in this simulation. In this paper, we will limit our findings to the Weighted Least Norm solution control. Five different values are being tried for the diagonal elements of the weight matrix (W_d) to implement the control system and to verify its effectiveness. Figure 8 shows the initial pose of the WMRA system at the beginning of the simulation, and Figures 9, 10, 11, 12 and 13 show the final poses of the WMRA system after the end-effector reached the desired destination for the five cases studied. The weight matrix of the first case carried in its diagonal elements the same value "1" for all 9 variables. That means that all seven joints of the arm and the two wheelchair's position and orientation variables will have equal potential of motion as shown if Figure 9. In the second case, W_d carried "10" for each of the arm's seven joints, and "1" for wheelchair's position and orientation variables, which means that the wheelchair's two variables are 10 times more likely to move than the arm's joints, and that is apparent in the results shown in Figure 10. The third case carried weights of "1" for the arm's joints, and "100" for the wheelchair's two variables in W_d, which means that the arm is 100 times more likely to move than the wheelchair, and that can be clearly seen in Figure 11, where the wheelchair had a minimal motion and the arm did most of it.

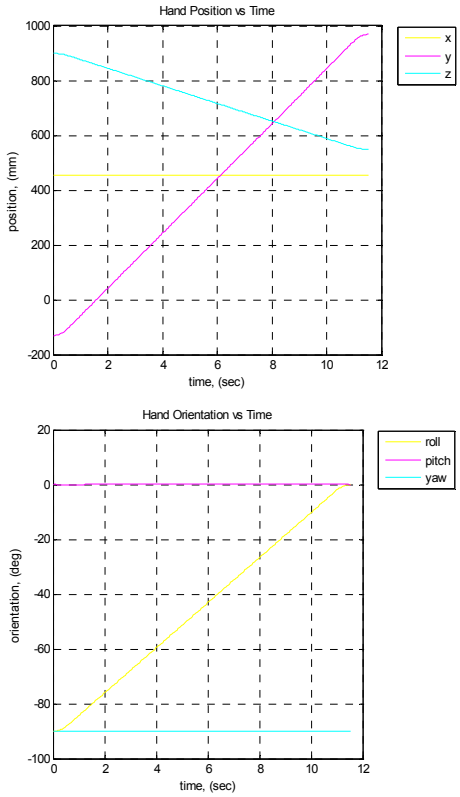

Figure 7: Position and orientation of the WMRA system during simulation

The beauty of this method comes apparent in the last two cases, where in the fourth case, W_d carried weights of "1" for the arm's seven joints and the wheelchair's orientation variable, and a weight of "100" for the wheelchair's position. This means that the pure forward or backward motion of the wheelchair is 100 times less likely than the motion of the rest of the system, and Figure 12 shows how the wheelchair's forward motion was minimal. Figure 13 shows the last case, which is the opposite of the fourth case, where the orientation of the wheelchair took a weight of "100", and the other eight variables took a weight of "1". This means that the wheelchair's rotational motion is 100 times less likely to occur than the than the motion in the arm's joints and the wheelchair's pure translational motion.

Figure 8: Initial pose of the WMRA system in simulation

Figure 9: Destination pose when Wd = [1, 1, 1, 1, 1, 1, 1, 1, 1]

Figure 10: Destination pose when Wd = [10, 10, 10, 10, 10, 10, 10, 1, 1]

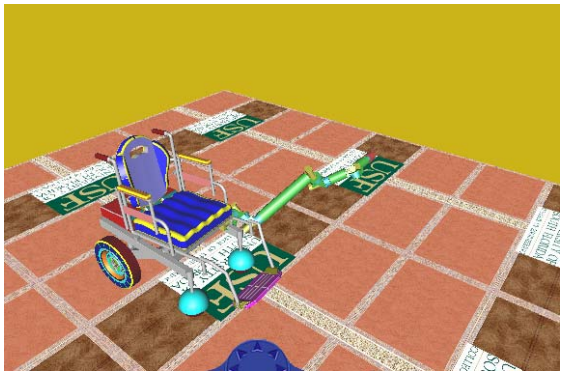

Figure 11: Destination pose when Wd = [1, 1, 1, 1, 1, 1, 1, 100, 100]

Figure 12: Destination pose when Wd = [1, 1, 1, 1, 1, 1, 1, 100, 1]

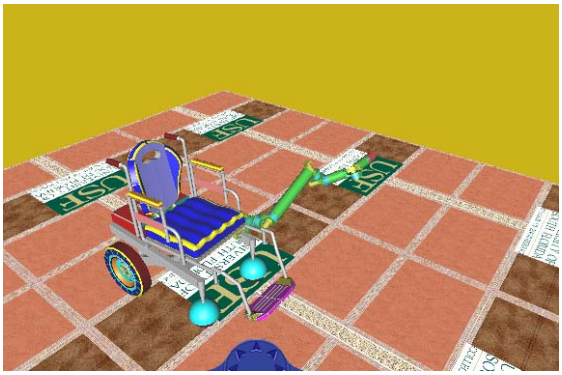

Figure 13: Destination pose when Wd = [1, 1, 1, 1, 1, 1, 1, 1, 100]

The simulation program is designed to give different useful values and plots throughout the simulation process for observation and diagnosis of any potential problems that might occur during the task execution whether the physical arm is running or just the simulation. Among these plots are the joints' angular displacements and velocities. Figures 14 through 18 show the angular displacement versus time for the arm's seven joints throughout the simulation period for all five cases. The first case in Figure 14 shows the normal weights with no preference to any of the nine variables. In the second case (Figure 15), when the arm carried a heavy weight in the weight matrix, it is clear that the seven arm joints had minimal motion that was necessary for the destination to be reached. That end-effector destination is impossible to reach by using the two wheelchair's variables only. The last three cases show an easy arm motion as compared to that of the wheelchair.

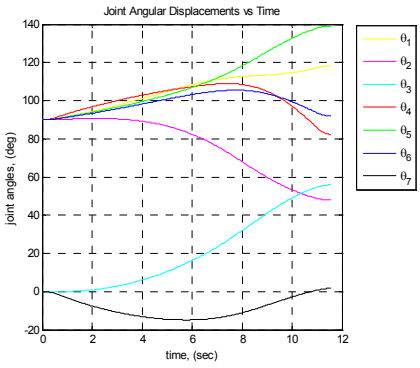

Figure 14: Arms' joint motion when Wd = [1, 1, 1, 1, 1, 1, 1, 1, 1]

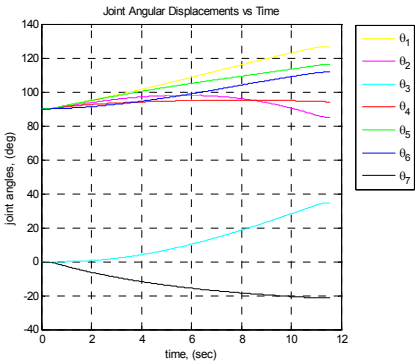

Figure 15: Arms' joint motion when Wd = [10, 10, 10, 10, 10, 10, 10, 1, 1]

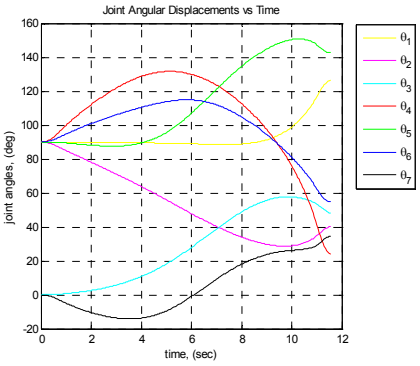

Figure 16: Arms' joint motion when Wd = [1, 1, 1, 1, 1, 1, 1, 100, 100]

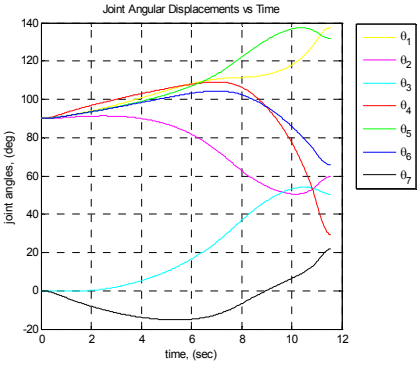

Figure 17: Arms' joint motion when Wd = [1, 1, 1, 1, 1, 1, 1, 100, 1]

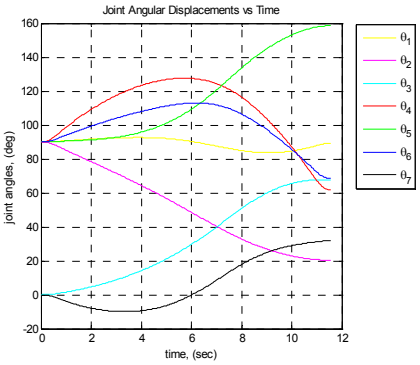

Figure 18: Arms' joint motion when Wd = [1, 1, 1, 1, 1, 1, 1, 1, 100]

Another plot that is given in the simulation program is the track distances drawn by each of the two wheels of the wheelchair. These plots are useful in particular to observe the wheelchair's motion. Figures 19 through 23 show these distances driven through the simulation for all five cases. An important property of this optimization method was apparent during simulation, and can be seen in Figure 19, which was minimization of singularity. As the arm was moving to the destination and the left wheel was moving backwards, that left wheel reversed it motion in the middle of the simulation period when the arm started approaching singularity as seen in Figure 24. The maximum wheelchair motion occurred in the second case as shown in Figure 20, where the weight was on the arm, and the wheelchair was free to move.

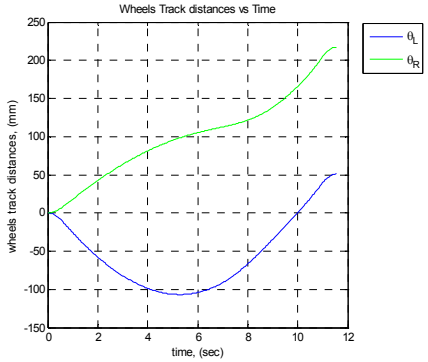

Figure19: Wheels' motion when Wd = [1, 1, 1, 1, 1, 1, 1, 1, 1]

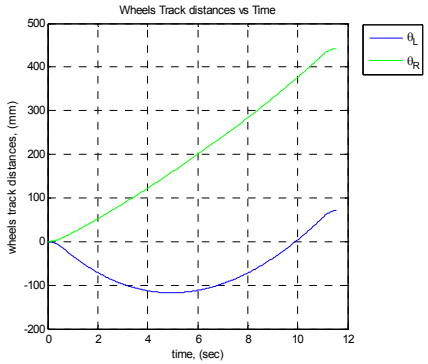

Figure 20: Wheels' motion when Wd = [10, 10, 10, 10, 10, 10, 10, 1, 1]

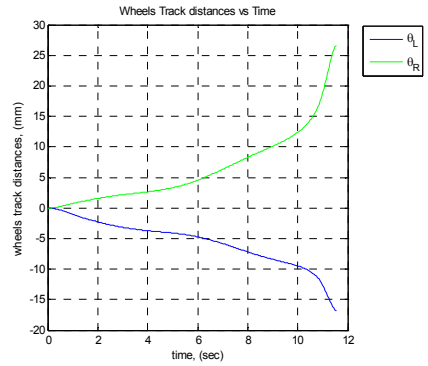

Figure 21: Wheels' motion when Wd = [1, 1, 1, 1, 1, 1, 1, 100, 100]

Figure 21 shows the opposite, where the wheelchair moved the least among all cases since the weight was on the wheelchair's motion and the arm was doing most of the motion to the destination. Figures 22 and 23 show how the opposite weights carried by the position & orientation variables of the wheelchair in these two cases lead to a pure rotation (figure 22) where both wheels carried the same but opposite motion, and a translation (Figure 23) where both wheels carried the same motion.

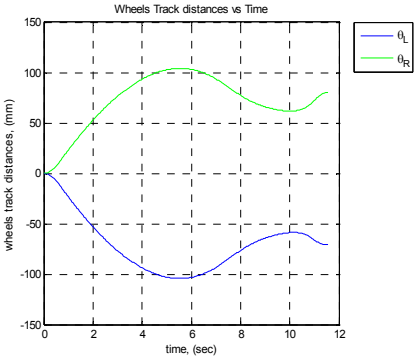

Figure 22: Wheels' motion when Wd = [1, 1, 1, 1, 1, 1, 1, 100, 1]

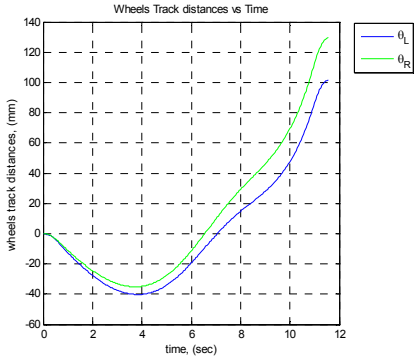

Figure 23: Wheels' motion when Wd = [1, 1, 1, 1, 1, 1, 1, 1, 100]

Figures 24 through 28 show the manipulability index of both the arm alone and the combined WMRA system. It is important to note here that these values are to be multiplied by (10^{-9}) to get the normalized manipulability measure. It is clear that the manipulability is much higher for the WMRA system than that of the arm only due to the fact that the WMRA system carries two more degrees of freedom.

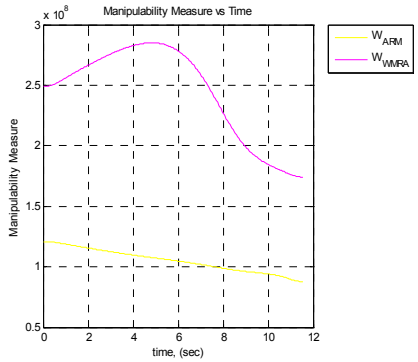

Figure 24: Manipulability index when Wd = [1, 1, 1, 1, 1, 1, 1, 1, 1]

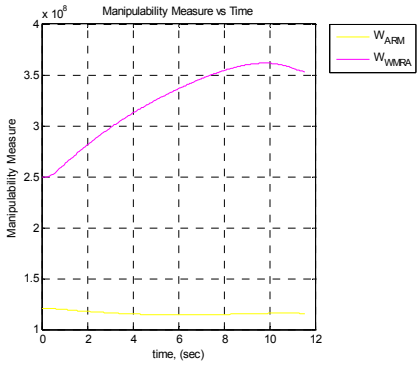

Figure 25: Manipulability index when Wd = [10, 10, 10, 10, 10, 10,10,1,1]

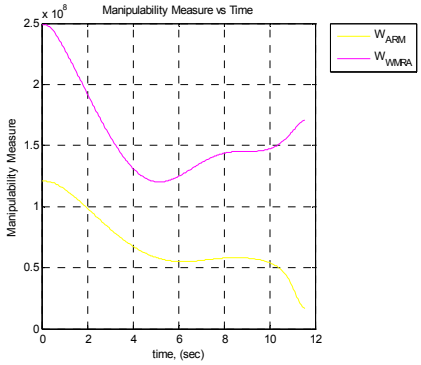

Figure 26: Manipulability index when Wd = [1, 1, 1, 1, 1, 1, 1, 100, 100]

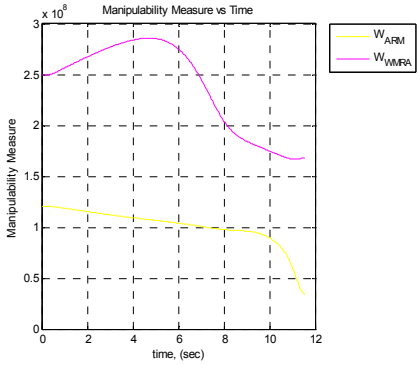

Figure 27: Manipulability index when Wd = [1, 1, 1, 1, 1, 1, 1, 100, 1]

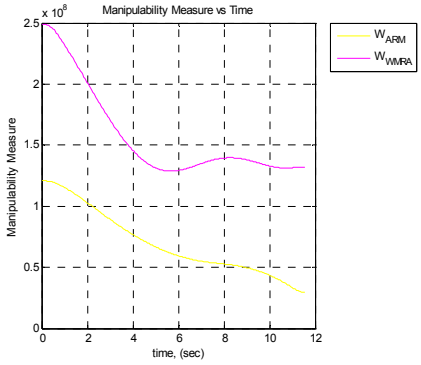

Figure 28: Manipulability index when Wd = [1, 1, 1, 1, 1, 1, 1, 1, 100]

In all five cases, the manipulability measure is maximized based on the weight matrix. Figure 25 shows the manipulability of the arm nearly constant because of the minimal motion of the arm. Figure 26 shows how the wheelchair started moving rapidly later in the simulation (see Figure 21) as the arm approached singularity, even though the weight of the wheelchair motion is heavy. This helped in improving the WMRA system's manipulability.

It is important to mention that changing the weights of each of the state variables gives motion priority to these variables, but may lead to singularity if heavy weights are given to certain variables when they are necessary for particular motions. For example, when the seven joints of the arm were given a weight of "1000" and the task required rapid motion of the arm, singularity occurred since the joints are nearly stationary. Changing these weights dynamically in the control loop depending on the task in hand leads to a better performance. This subject will be explored and published in a later publication. Figure 29 shows the WMRA system installed on the modified wheelchair "Action Ranger X Storm Series" with Barrett hand gripper, a camera and a Space Ball user interface.

Figure 29: WMRA system in testing

6. CONCLUSIONS AND FUTURE WORK

A wheelchair-mounted robotic arm (WMRA) was designed and built to meet the needs of mobility-impaired persons, and to exceed the capabilities of current devices of this type. Combining the wheelchair control and the arm control with the augmentation of the jacobian to include representations of both jacobians resulted in a control system that effectively and simultaneously controls both devices at once. The mechanical design incorporates DC servo drive with actuators at each joint, allowing reconfigurable link lengths and thus greater adaptability to a range of workspaces. Nine principal degrees of freedom allow full pose control of both the wheelchair and the arm. The control system is designed for coordinated Cartesian control with singularity robustness and task-optimized combined mobility and manipulation. Weighted Least Norm solution is implemented among others for preference control of each of the joints and the wheelchairs' position and orientation.

Modularity in both the hardware and software levels allows multiple input devices to be used to control the system. Testing the new system with human subjects with disabilities will be conducted after making the proper safety measures and under the supervision of the VA and Shriners Children hospital. More future developments include the use of remote controlled devices with an LCD screen to control the wheelchair-arm system from a remote location. This enables the user with disabilities to perform different tasks without the need to be on the wheelchair.

7. REFERENCES

[1] US Census Bureau (1997), "Disabilities affect one-fifth of all americans," *Census Brief* , CENBR/97-5, December 1997, http://www.census.gov/prod/3/97pubs/cenbr975.pdf

[2] Reswick J.B., "The moon over dubrovnik - a tale of worldwide impact on persons with disabilities," *Advances in External Control of Human Extremities*, 1990.

[3] Holly A. Yanco., "Integrating robotic research: a survey of robotic wheelchair development," *AAAI Spring Symposium on Integrating Robotic Research*, Stanford, California, March 1998.

[4] H.Eftring, K.Boschian, "Technical results from manus user trials," *Proc. ICORR* '99, 136-141, 1999.

[5] R. M. Mahoney, "The Raptor wheelchair robot system", *Integration of Assistive Technology in the Information Age.* Pp. 135-141, IOS, Netherlands, 2001.

[6] T.F. Chan, R.V. Dubey, "A Weighted Least-Norm Solution Based Scheme for Avoiding Joint Limits for Redundant Joint Manipulators". *1995 IEEE Robotics and Automation Transactions (R&A Transactions 1995).* Vol. 11, Issue 2, pp. 286-292, April, 1995

[7] J. Chung, S. Velinsky, "Robust Interaction Control of a Mobile Manipulator - Dynamic Model Based Coordination". *1999 Journal of Intelligent and Robotic Systems*, Vol. 26, No. 1, pp. 47-63, 1999.

[8] M. Galicki, "Control-Based Solution to Inverse Kinematics for Mobile Manipulators Using Penalty Functions". *2005 Journal of Intelligent and Robotic Systems*, Vol. 42, No. 3, pp. 213-238, 2005.

[9] A. Luca, G. Oriolo, P. Giordano, "Kinematic Modeling and Redundancy Resolution for Nonholonomic Mobile Manipulators". *Proceedings of the 2006 IEEE International Conference on Robotics and Automation (ICRA 2006)*, pp. 1867-1873, May, 2006.

[10] E. Papadopoulos, J. Poulakakis, "Planning and Model-Based Control for Mobile Manipulators". *Proceedings of the 2000 Conference on Intelligent Robots and Systems (IROS 2000)*, 2000.

[11] R.M. Alqasemi, E.J. McCaffrey, K.D. Edwards, R.V. Dubey, "Analysis, evaluation and development of wheelchair-mounted robotic arms," *Proc. ICORR '05,* Chicago, IL, June 2005.

[12] Craig, J., 2003, "Introduction to robotics mechanics and control", third edition, Addison- Wesley Publishing, ISBN 0201543613.

[13] Yoshikawa, T., 1990, "Foundations of robotics: analysis and control", MIT Press, ISBN 0262240289.

[14] Nakamura, Y., 1991, "Advanced robotics: redundancy and optimization", Addison- Wesley Publishing, ISBN 0201151987.

[15] K. Edwards, R. Alqasemi, R. Dubey, "Design, construction and testing of a wheelchair-mounted robotic arm," *Proc ICRA '06,* Orlando, FL, May 2006.